CHALMERS

Coverage Analysis and Cooperative Hybrid Precoding for 5G Cellular Networks

CHAO FANG

Communication Systems Group
Department of Electrical Engineering
CHALMERS UNIVERSITY OF TECHNOLOGY
Gothenburg, Sweden 2019

Thesis for the degree of Licentiate of Engineering

Coverage Analysis and Cooperative Hybrid Precoding for 5G Cellular Networks

Chao Fang

CHALMERS

Communication Systems Group
Department of Electrical Engineering
Chalmers University of Technology

Gothenburg, Sweden 2019

Fang, Chao
Coverage Analysis and Cooperative Hybrid Precoding for 5G Cellular Networks.

Department of Electrical Engineering
ISSN 1403-266X

Communication Systems Group
Department of Electrical Engineering
Chalmers University of Technology
SE-412 96 Göteborg, Sweden
Telephone: + 46 (0)723536379
Email: fchao@chalmers.se

This thesis has been prepared using LaTeX.

Printed by Chalmers Reproservice,
Göteborg, Sweden, June 2019.

To my parents and Suyang

Abstract

5G innovations have been made in both the network deployment and the transceiver architectures in order to increase coverage, energy- and spectrum-efficiency. Future base stations (BSs) are expected to be densely deployed in places such as walls and lamp posts and cover a smaller area compared to current macro BS systems. Using large spectrum at millimeter-wave (mmWave) frequency bands and highly directional beamforming with large antenna arrays, 5G will bring gigabit-per-second data rate and low-latency communications and enable many novel services such as high-speed mmWave wireless interconnections between devices, vehicular communications, etc.. Moreover, mmWave communication systems will be based on novel hybrid beamforming architectures which have reduced hardware power consumption and cost. Thus, for better understanding of 5G performance and limitations, one of the main goals in this thesis is to analyze new models that give tractable performance metrics for dense small BS networks. Another goal in this thesis is to study mmWave hybrid beamforming schemes which enable joint transmissions in multi-cell multi-user systems. In the thesis, we show the advantages of small cells in increasing the coverage probability and reducing the path loss and shadowing, and we show the value of cooperation in terms of power consumption and outage.

In [Paper A] we derive analytical expressions for the successful reception probability of the equal gain combining receiver in a network where interfering transmitters are distributed according to a Poisson point process and interfering signals are spatially correlated. The results show that the spatial correlation reduces the successful reception probability and the effect of the spatial correlation increases with the number of antennas. [Paper B] follows to study the performance of a partial zero forcing receiver. The results are simulated in an environment with blockages and are analyzed under both Rayleigh and Rician channels. The coverage probability is shown to be maximized when using a subset of antennas' degree-of-freedom for useful signal enhancement and using the remaining degrees of freedom for canceling the interference from strongest interferers. Finally, in [Paper C], we propose a hybrid beamforming scheme which minimizes the total power consumption of a multi-cell multi-user network, subject to per-user quality-of-service constraints. The proposed scheme is based on decoupling the analog precoding and digital precoding. The analog precoders are only dependent on the local channel state information at each BS. Then, the digital precoders are obtained by solving a relaxed convex optimization for given analog precoders. Simulation results show that the proposed algorithm leads to almost the same RF transmit power as that of fully digital precoding, while saving considerable hardware power due to the reduced number of RF chains and digital-to-analog converters.

Keywords: millimeter wave, heterogeneous networks, beamforming, 5G.

List of Included Publications

The thesis is based on the following appended papers:

[A] C. Fang, B. Makki, X. Xu and T. Svensson, "Equal gain combining in Poisson networks with spatially correlated interference signals," in *IEEE Wireless Commun. Letters*, vol. 5, no. 6, pp. 628-631, Dec. 2016.

[B] C. Fang, B. Makki and T. Svensson, "Coverage analysis for millimeter wave uplink cellular networks with partial zero-forcing receivers," in *International Symposium on Modeling and Optimization in Mobile, Ad Hoc, and Wireless Networks (WiOpt)*, Paris, 2017, pp. 1-6.

[C] C. Fang, B. Makki, J. Li and T. Svensson, "Coordinated hybrid precoding for energy-efficient millimeter wave systems," in *IEEE International Workshop on Signal Processing Advances in Wireless Communications (SPAWC)*, Kalamata, 2018, pp. 1-5.

Acknowledgements

I would first like to thank my main supervisor Prof. Tommy Svensson for his invaluable expertise in formulating the research topics and the opportunities I was given to collaborate with and gain knowledge from good researchers globally. His advice on the direction and management of my research life will help me greatly in furthering my research in the future. I would like to thank my co-supervisor Dr. Behrooz Makki for his insightful comments on the manuscripts and spending time to give me guidance.

I would like to thank Dr. Jingya Li from Ericsson and formerly our group, you are always willing to help and I learned a lot from you during our fruitful discussions. I would like to acknowledge Prof. Xiaodong Xu from BUPT for his valuable guidance and support during my master study and in the beginning of my PhD study. Many thanks to the head of our division, Prof. Erik Ström, and the head of our group, Fredrik Brännström, for ensuring a stimulating and joyful research atmosphere.

I would also like to thank all current and former colleagues of the communication systems group for creating a pleasant working environment. In particular, I would like to thank my former officemates Christopher, Naga, and Srika, for providing all the useful information and advice to a new-comer, and my current officemate Jesper, for the interesting discussions and playing nice music all day in the office. Also, many thanks to the administrative staff for all their help. Special thanks to the current and former members of the Chinese "mafia" in the group, Chenjie, Hao, Li, Wei, Wanlu, Xinlin, Xiaoming, Yutao, Yuxuan, and Zhenhua, for the good time we have had.

My deepest thanks go to my parents and my wife Suyang for being always there for me.

Chao Fang
Göteborg, June 2019

This work has been supported in part by the Swedish Governmental Agency for Innovation Systems (VINNOVA) within the VINN Excellence Center Chase/ChaseOn and the European Commission H2020 programme under grant agreement n° 671650 (5G PPP mmMAGIC project).

Acronyms

2/3/4/5G:	Second/third/fourth/fifth generation
3GPP:	3rd Generation Partnership Project
BS:	Base stations
CCDF:	Complementary cumulative distribution function
CoMP:	Coordinated multi-point
CSI:	Channel state information
DAC/ADC:	Digital-to-analog/Analog-to-digital converters
ITU:	International Telecommunication Union
LTE:	Long term evolution
LOS:	Line-of-sight
MmWave:	Millimeter wave
MIMO:	Massive-input massive-output
NLOS:	Non-line-of-sight
QoS:	Quality-of-service
RF:	Radio frequency
SINR:	Signal-to-interference-plus-noise ratio

Contents

Abstract i

List of Included Publications iii

Acknowledgements v

Acronyms vii

I Overview 1

1 Introduction 1
- 1.1 Background and Motivation . . . 1
- 1.2 Aim of Thesis . . . 3
- 1.3 Organization of Thesis . . . 3
- 1.4 Notation . . . 4

2 Poisson Networks 5
- 2.1 Interference Characterization . . . 5
- 2.2 Cell Association . . . 6
- 2.3 SINR Characterization . . . 7

3 Coordinated Multi-Point mmWave Systems 9
- 3.1 Downlink CoMP Categories . . . 10
- 3.2 Joint Hybrid Precoding in Cooperative MmWave Systems . . . 11
  - 3.2.1 System Model . . . 11
- 3.3 MmWave Channel Model . . . 14

4 Conclusions and Future Work 16
- 4.1 Contributions . . . 16
- 4.2 Future Work . . . 17
- 4.3 List of Related Publications . . . 17

References 19

II Included papers **23**

A Equal Gain Combining in Poisson Networks With Spatially Correlated Interference Signals **A1**
1 Introduction . . . A2
2 System Model . . . A2
3 Successful Reception Probability . . . A3
3.1 EGC with N Receive Antennas . . . A5
3.2 Area Spectral efficiency . . . A7
4 Simulation Results . . . A8
5 Conclusion . . . A9

B Coverage analysis for millimeter wave uplink cellular networks with partial zero-forcing receivers **B1**
1 Introduction . . . B2
1.1 Contributions . . . B2
2 System Model . . . B3
3 Uplink Coverage in mmWave Networks . . . B5
3.1 Laplace Transform of the Interference Power . . . B5
3.2 General Coverage Probability . . . B7
3.3 Upper Bound for the Coverage Probability . . . B8
4 Simulation Results . . . B9
5 Conclusion . . . B11

C Coordinated Hybrid Precoding for Energy-Efficient Millimeter Wave Systems **C1**
1 Introduction . . . C2
2 System Model . . . C3
3 Joint Hybrid Precoding Problem Formulation . . . C4
3.1 Anlog Precoder Design Using Equal Gain Transmission . . . C5
3.2 Digital Precoder Design . . . C6
4 Simulation Results . . . C8
5 Conclusion . . . C11

Part I

Overview

Chapter 1

Introduction

1.1 Background and Motivation

Modern telecommunications evolving from second generation (2G) networks to long term evolution (LTE) and onwards to fifth generation (5G) networks have changed our lifestyle completely. In 2G, the first digital communication systems was implemented and many data services that we are used to now such as SMS text messages were introduced. In third generation (3G), the internet speed was significantly improved and audio and video streaming became available to mobile phone users for the first time. Then, LTE, developed by 3GPP, further enhanced data rate and reduced the latency, enabling applications including Voice over Internet Protocol and video conferencing. Today, due to the proliferation of connected devices and the growth of Internet of Things, the demand for even higher data rate and better energy efficiency drives researchers and industry to develop 5G which is expected to generate 3 times or more traffic than average 4G connections [1] and achieve more than 1 gigabit per second data rate. The main features of 5G include using high bandwidth (greater than 1 GHz) at millimeter (mmWave) frequency spectrum and massive number of antennas for better energy efficiency, broader coverage and low latency (on the order of about 1 ms) [2–5]. In order to formally define the 5G standard, International Telecommunication Union (ITU) set up the IMT-2020 requirements [6] and 3GPP recently started preparing the sumbmission of technologies for IMT-2020 [7]. Also, many measurements campaigns were conducted in indoor and urban outdoor scenarios to provide data on various channel characteristics and help developing accurate statistical channel models [8, 9, 15].

Due to the fact that the spectrum below 6 GHz used by current communication systems is fully occupied, 5G will utilize the mmWave spectrum in order to increase the channel bandwidth. The main reason why mmWave spectrum was considered unsuitable for mobile communications is the high path loss, rain and atmospheric absorption which greatly limits the transmission range. Today, technologies such as mmWave low-cost CMOS circuitry and high-gain miniaturized antennas have made mmWave more practical than before [4]. The small wavelength allows building high gain antenna arrays on a small-scale chip, which will help counter the higher propagation loss associated

with high frequency signals. The main challenge now becomes how to efficiently use multiple-input-multiple-output (MIMO) techniques to create directional beamforming maximizing the energy and spectrum efficiency. Since massive antenna arrays are likely to be employed in 5G, the conventional digital beamforming architecture which requires a complete radio-frequency (RF) chain for each antenna is considered too costly. Most research concerning mmWave beamforming schemes have adopted alternative architectures including the hybrid architecture [2, 7, 13], the switch based architecture [8] and low-precision analog-to-digital converters (ADCs) [15] in order to reduce the cost on the hardware. In a single cell setup, it has been shown that these alternative architectures can achieve high data rate close to that of the fully digital architecture by exploiting the spatial multiplexing gains [2, 3, 7, 8, 13]. For multi-cell and multi-user setups, the joint user selection and coordinated multipoint (CoMP) transmissions between base stations (BSs) are excellent techniques to achieve high spectrum efficiency and make the network robust to the change of channel conditions. However, there has only been very limited research about coordinated hybrid beamforming in multi-cell mmWave networks. In [17], the user-beam selection problem where BSs jointly select directional beams and users in order to maximize the users' rates is studied. Considering multiple cells and pre-associated users, hybrid precoding methods maximizing the per-user signal-to-interference-plus-noise ratio (SINR) are proposed in [18]. Full coordination among BSs that allows multiple streams transmitting jointly from multiple BSs to a single user is missing in the context of hybrid precoding for mmWave systems. Thus, hybrid beamforming for joint transmissions is an interesting research topic as it can help determine what coordinated beamforming strategy gives the largest performance gains in mmWave systems.

Due to the high path loss and penetration loss, mmWave signals have limited transmission range. For thie reason, 5G networks will be heterogeneous and consist of BSs with different carrier frequencies, cell range and backhaul methods [19, 20]. The requirements and enhancements of small cells have been studied by standardization bodies such as 3GPP for exiting network infrastructures [21]. The evolution of BSs for 5G systems is still under discussion, but it is clear that 5G BSs will be equipped with hundreds of antennas, which are integrated in a small-scale chip due to the small wavelength of mmWave frequency signals, and use direction beamforming between users and BSs to achieve larger signal power and better interference management. Also, 5G BSs will be placed closer to the users, such as on lamp posts, walls, ect., in order to facilitate line-of-sight (LOS) transmissions and eliminate high installation and rental costs.

The main benefit of heterogeneous networks is the reduction of competition for resource blocks at each BS and high network throughput [2]. But the drawback is the increase of inter-cell interference and the backhaul from small cells to the core. As the network topology becomes irregular and opportunistic, small BSs can be deployed close to macro BSs with overlapped coverage area and spectrum. This deployment can cause significant interference to small-cell users in the uplink or cell-edge macro-cell users in the downlink. Mechanisms such as user scheduling, power control, frequency assignment and coverage optimization are important research topics for interference management [19]. In addition, providing backhual to dense small cells can be a costly and complex problem if using wired backhual. To address this problem, integrated access and backhaul, where mobile users and backhaul links share the same wireless channel are considered

for 5G BSs [22–24]. Another challenge for heterogeneous networks is the cell association. As a result of various cell transmit power and the presence of blockages, the strongest radio propagation path may not come from the nearest BS. How to associate a user to a strong BS and balance the traffic load between BSs are important issues in heterogeneous networks [25]. Furthermore, for moving users, handovers involving small BSs presents some unique challenges. Because the small BSs are massively deployed, the amount of handovers increases and neighboring BSs may not be updated properly. Therefore, it is crucial to develop low-delay handover strategies between different tiers.

1.2 Aim of Thesis

The aim of the thesis is to provide analytical tools to assess the performance of heterogeneous and mmWave networks. We derive analytical expressions for the coverage probability of heterogeneous networks and propose cooperative hybrid precoding methods in cooperative mmWave networks. The analysis of the effect of various network parameters, such as the number of antennas and network density, on the received signal quality provides useful insights into the network design. From simulation results, we conclude that the analytical expressions can provide accurate coverage probability with reduced computation complexity compared to Monte Carlo based link-level simulations. Moreover, we show that cooperative mmWave networks with hybrid precoding can largely reduce the power consumption while satisfying the per-user minimum rate constraints.

In paper A, we focus on the distribution of SINR, which is the fundamental metric to characterize the coverage probability, for a receiver based on equal-gain combining. We show the effect of interference correlation on the SINR distribution due to the spatial locations of the interfering transmitters. In paper B, we analyze the coverage probability of the partial-zero-forcing receiver for a mmWave network. Considering the blocking effect, we give insights on the optimal scheme between interference management and useful signal enhancement which maximizes the coverage probability. In paper C, we present a joint hybrid precoding scheme minimizing the total power consumption in a cooperative mmWave system subject to per-user spectral efficiency constraints. We define a realistic power consumption model which takes the hardware components used in the architectures and the BSs' activation modes into consideration. The power consumptions are studied under different cooperative network sizes as well as different blocking conditions to provide the value of joint precoding in multi-cell mmWave networks.

1.3 Organization of Thesis

The thesis is organized as follows. We introduce the modeling of dense networks and characterize the interference and SINR distributions in Chapter 2. In Chapter 3, we explain the settings of a cooperative mmWave system. Finally, Chapter 4 summarizes our contributions in the appended papers.

1.4 Notation

This section shows the notation used in Part I of the thesis. We use bold lower-case letters like $\mathbf{d}$ for vectors and upper-case bold letters like $\mathbf{R}$ for matrices. Then, $\mathbf{R}^T$, $\mathbf{R}^H$, $\mathbf{R}^{(i,j)}$ and $||\mathbf{R}||_F$ denote the transpose, the Hermitian, the (i,j)-th entry of $\mathbf{R}$ and the Frobenius norm of $\mathbf{R}$, respectively. $\mathbb{C}^n$ represents the set of n-tuples of complex numbers represented as column vectors and $\mathbb{C}^{m\times n}$ denotes the set of complex $m \times n$ matrices.

Chapter 2

Poisson Networks

In this chapter, we concentrate on networks where the transmitters are distributed based on a Poisson point process (PPP). The PPP is used in most of the analytical work on unstructured dense network characterization and allows for increased tractability on key performance metrics.

2.1 Interference Characterization

Due to the scarcity of the spectrum in current cellular systems and the roll-out of small cells, inevitably, the received signal is subject to additive noise and undesired signals from other interfering transmitters. Although inter-cell interference can be managed through frequency reuse or coordinated multi-cell transmissions, it is limited by the cell size and is generally impossible to achieve per-link level interference elimination in dense networks [26], e.g., sensor networks, cognitive networks and heterogeneous networks. The path loss law states that the signal power scales with distance, therefore the interference power will be more severe in dense networks, which makes studying the statistics of interference power critical.

Consider a receiver y and a set of transmitters, $\mathcal{X} = \{x_i\}_{i=1}^{N}$ that are distributed in a 2-dimensional plane. At a given time instant, a set of active transmitters, $\Phi \subseteq \mathcal{X}$, causes interference to y. For single antenna systems, the interference power at y is given by

$$I = \sum_{x_i \in \phi} P_{x_i} |h_{x_i}|^2 \ell\left(||x_i - y||\right), \tag{2.1}$$

where P_{x_i} denotes the transmit power of transmitter x_i, $|h_{x_i}|^2$ the fast fading power in the x_i-y link, $\ell(\cdot)$ the path loss function and $||x_i - y||$ the distance between x_i and y. In (2.1), the randomness comes from the fast fading and the geometry of the interfering transmitters. Since the signal power is largely affected by the path loss, depending on the distance between the transmitters and the receivers, the distribution of the transmitters determines the strength of the interference power. The interference power is often

characterized by its Laplace transform

$$\mathcal{L}_I(s) = \mathbb{E}\left[\exp(-sI)\right]. \tag{2.2}$$

For deterministic networks, where the locations of transmitters are at the centers of lattices, the Laplace transform can be found in closed form as in [27]. For unstructured and dense networks, the transmitters locations are well modeled by a PPP [26–28], which assumes the transmitters are randomly placed with a uniform distribution in the plane. Denote the intensity of interfering transmitters by λ. Then, using tools from stochastic geometry, the Laplace transform of the interference power is given by [27, Eq. (3.20)]

$$\mathcal{L}_I(s) = \exp\left(-\lambda\pi\mathbb{E}[|h|^{4/\alpha}]\Gamma(1-2/\alpha)s^{2/\alpha}\right), \tag{2.3}$$

where we have assumed unit transmit power and the path loss law $\ell(r) = r^{-\alpha}$ with α denoting the path loss exponent. The Laplace transform (2.3) has a closed-form expression in the case of Rayleigh fading, $\mathbb{E}\left[|h|^{4/\alpha}\right] = \Gamma(1+2/\alpha)$. As shown in the following, knowing the Laplace transform of the interference power helps to derive the distribution of the SINR.

2.2 Cell Association

Cell association strategies seek the serving BS for a user based on SINR related metrics. The decisions are usually made based on link quality, traffic load requirements and location information. In heterogeneous networks, by offloading users to nearby small BSs while actively controlling the resource block of the macro BS to be blank, users can have a much larger SINR from small BSs [29]. Due to the difference in coverage area, transmit power, antenna sizes and antenna gains between macro and small BSs, decoupling the uplink and downlink allows users to find the best interference environment for the two links independently. By giving different association biases to uplink and downlink BSs, it has been shown that the joint uplink-downlink coverage probability can be maximized [30]. However, decoupled schemes make the channel of both directions not reciprocal due to different locations and hardware of the uplink and downlink BSs, thus requiring additional channel training in time-division-duplex systems. Another challenge for decoupled schemes is how to allow a fast exchange of control information between uplink and downlink BSs. In mmWave systems, it may be beneficial to associate a user to a mmWave small cell in the downlink for the high data rate, while sending uplink signals to a sub-6GHz macro cell for robust link quality.

The simplest cell association strategy associates a user to the nearest BS. If the path loss model is given by $\ell(r) = r^{-\alpha}$, the nearest BS association gives the maximum signal power averaged over fading. Figure 2.1 shows the coverage area of a heterogeneous network with large cells and small cells. Based on the nearest BS association, the coverage area forms a Voronoi tessellation where the boundaries have equal average received power from the nearest BSs. In order to achieve better load balance between macro and small BSs, a bias factor can be added to the average received power model given by $B_i P_i r^{-\alpha_i}$, where B_i represents the bias towards associating to i-th tier BSs. Thus, by associating

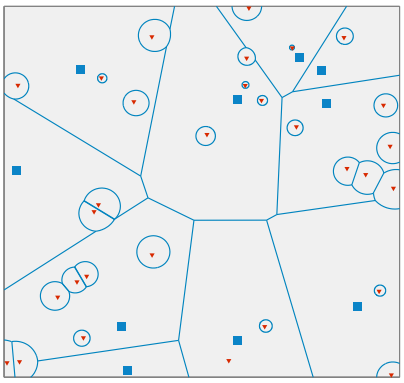

Figure 2.1: A realization of a heterogeneous network consisting of macro BSs and small BSs. The blue squares and red triangles denote the macro and small BSs with descending transmit powers, respectively.

users to the BS with the maximum biased received power averaged over fading, small BSs' coverage area can be expanded through increasing the bias factor, thus offloading to small BSs. However, if we include the blocking effect, the nearest BS does not necessarily provide the highest signal strength and serving a user by a BS with line-of-sight (LOS) connection may lead to better system performance.

2.3 SINR Characterization

The SINR for a receiver at the origin of a 2-dimensional plane with single antenna on both the transmitter and the receiver sides is given by

$$\text{SINR} = \frac{\ell(r_0)|h_0|^2}{\sum_{k\in\Phi,k\neq 0}\ell(r_k)|h_k|^2+\sigma^2}, \tag{2.4}$$

where r_0 denotes the distance to the associating BS, Φ is the set of interfering BSs which are assumed to be distributed according to a PPP with intensity λ and r_k represents the distance to the k-th interfering BS. Also, $|h_0|^2, |h_k|^2$ are the fast fading scaling factor for the useful signal link and the k-th interfering link, respectively, and σ^2 is the additive noise power. Assuming the nearest BS association strategy, the path loss model $\ell(r_0) = r_0^{-\alpha}$ and $|h_0|^2 \sim \text{Exp}(1/\mu)$ where μ denotes the constant transmit power, closed-form expression of the SINR complementary cumulative distribution function (CCDF), which is the probability of coverage for a given SINR threshold T, is obtained as [26, Eq. (2)]

$$\mathbb{P}\left(\text{SINR} > T\right) = \int_{r>0} \exp\left(-\lambda\pi r^2 - \mu T r^{\alpha}\sigma^2\right)\mathcal{L}_I\left(\mu T r^{\alpha}\right)2\pi\lambda r \mathrm{d}r. \tag{2.5}$$

Significant simplification of (2.5) can be made if the interference power also follows the exponential distribution and the system is interference-limited, and the simplified expression is given by [26, Eq.(11)]

$$\mathbb{P}\left(\text{SINR} > T\right) = \frac{1}{1 + T^{2/\alpha} \int_{T^{-2/\alpha}}^{\infty} \frac{1}{1+u^{\alpha/2}} \mathrm{d}u}. \tag{2.6}$$

Hence, for Poisson networks, we see that tractable expressions for the SINR distribution can be derived and does not require Monte Carlo simulations.

For multi-antenna systems, the post processing SINR after the receiver combining becomes more difficult to characterize. In paper A, we focus on the equal gain combiner with N receive antennas which co-phases the useful signals before combining and, consequently, the output signal benefits from the diversity gain. After combining, the SINR is given by

$$\text{SINR} = \frac{P_0 \left(\sum_{i=1}^{N} |h_i|\right)^2 \ell(r_0)}{\sum_{i=1}^{N} \sum_{x_i \in \Phi_i} P_{x_i} \ell(r_{x_i}) |h_{i,x}|^2 + \sigma^2}, \tag{2.7}$$

where Φ_i denotes the set of interfering transmitters picked up by the i-th antenna and P_0, P_{x_i} are the transmit power of the associated BS and the interfering BSs, respectively. In (2.7), it is assumed that each antenna receives interference from a fraction of the total interfering transmitters $\Phi_i \subseteq \Phi$. Despite of the independent fast fading, the interfering signals received on different antennas are correlated due to the fact that the spatial locations of some transmitters appear in different sets Φ_i. As we shall see in Paper A, the spatial correlation causes loss in the diversity gain. Note that the fading scaling factor after combining $\left(\sum_{i=1}^{N} |h_i|\right)^2$ no longer has a simple distribution form, hence, in Paper A, we give a tight approximation of the SINR distribution for any number of receive antennas [Paper A, Eq.(17)] and the exact expression for the case of two antennas [Paper A, Eq.(2)]. In Paper B, we study the partial-zero-forcing receiver which cancels some of the strongest interference signals and uses the remaining degrees of freedom of the antennas for useful signal enhancement. The received SINR for the partial-zero-forcing receiver is given by

$$\text{SINR} = \frac{P_0 |\mathbf{v}_0^H \mathbf{h}_0|^2 \ell(r_0)}{\sum_{k=K+1}^{\infty} P_k \ell(r_k) |\mathbf{v}_0^H \mathbf{h}_k|^2 + \sigma^2}, \tag{2.8}$$

where $\mathbf{v}_0, \mathbf{v}_k$ denote the combining weights at the receiver for the associating BS and the interfering BSs, respectively. Here, the interfering transmitters are sorted in a descending order in terms of the average received power. The partial-zero-forcing eliminates the K strongest interferers while maximizing the useful signal power. The SINR distribution for the partial-zero-forcing receiver is given by [Paper B, Eq.(16)].

Chapter 3

Coordinated Multi-Point mmWave Systems

The paradigm shift to heterogeneous networks is a clear sign that CoMP transmissions will play an important role in 5G cellular systems. Due to the large quantity of devices and BSs, strong inter-cell and intra-cell interference are the main performance limiting factors in downlink transmissions. Therefore, CoMP transmissions which coordinate the interference and the transmit signal power in multiple geographically separated BSs is required to achieve satisfying performance for all users in the network. In LTE, the intra-BS CoMP scenarios with ideal backhaul are defined in 3GPP release 11 [31] and the extension to inter-BS CoMP scenarios with non-ideal backhaul are defined in Release 12 [32]. Permitting cooperation among BSs and users achieves better resource utilization by transmitting data from BSs with low load, and joint reception from multiple BSs enhances the overall SINR and reduces the number of dropped connections. Therefore, there has been extensive research about jointly designing beamforming methods in coordinated MIMO systems to optimize the system spectrum and energy efficiency [9, 33, 35].

For mmWave networks, the CoMP design is more challenging. Due to the implementation of the hybrid architecture where each antenna is connected through phase shifters to a small number of RF chains, both analog and digital precoders need to be jointly designed. There are additional constraints on the hybrid architecture since the analog precoders are implemented by the phase shifters, compared to the fully digital architecture where only digital precoders are considered. Early work on the topic of joint hybrid beamforming design in mmWave systems are based on predefined beam patterns [17, 36]. The performance can be improved by calculating both the analog and digital precoders according to some performance metrics, which allows the beams to point at every direction.

In this chapter, we introduce the categories of CoMP transmission schemes in mmWave cellular systems. In particular, we present the modeling of a joint hybrid beamforming method in the multi-user and multi-BS setup. The hybrid beamforming scheme optimizes the power consumption of a heterogeneous network and yields the user association

that satisfies the rate requirement, which is the main contribution in Paper C.

3.1 Downlink CoMP Categories

For downlink multi-cell cooperation, it is often required that the BSs are mutually connected or connected to a central processing node, therefore channel information can be gathered from all BSs to make joint decisions on transmitting parameters such as user scheduling, beamforming precoders, transmit power, ect.. Based on the availability of the transmit data at the cooperating BSs and the type of BSs, CoMP communications can be categorized into the following categories [31, 37, 38]:

- *Coordinated scheduling/beamforming*: Each user is served by only one BS and transmit data corresponding to a given user is not required to be available for other BSs. The decisions on the user scheduling/beamforming are made according to the channel state information (CSI) of both direct and interfering links such that the system quality-of-service (QoS) is satisfied.
- *Joint processing*: Each user is allowed to be served by more than one BS, the joint processing is a more powerful tool which allows for simultaneous data transmission from multiple BSs to a single user, such that the received signal quality is improved. In this case, the transmit data for that user should be available at multiple BSs and multiple data streams transmitted from different BSs are combined coherently or non-coherently at the user side [39]. The joint processing using antennas belonging to different BSs is similar to the transmission in a MIMO channel, hence this scheme is also called *network MIMO*. Another type of joint processing, *dynamic point selection*, restricts the data to be transmitted from one BS in a time-frequency resource, but the transmitting BS is dynamically selected within the cooperating BSs in each subframe, and the data should also be available to multiple BSs.
- *Relay-assisted cooperation*: In contrast to cooperation among BSs, the relay-assisted cooperation adds dedicated relay nodes inside a cell and does not need connections to other BSs. The transmit data are firstly received and processed at a relay node before forwarding to the user. The simplest cooperation is the amplify-and-forward type which, however, amplifies both the useful signal power and the interference plus noise power. More advanced relay nodes decode and further process the data, such as data concatenation/segmentation, before encoding and forwarding to the user. This type of cooperation allows more control functions at the relay node and does not amplify the interference and the noise.

The theoretical studies of CoMP aim at optimizing the beamforming gains and the user association such that the users' QoS is improved. CoMP schemes not only can schedule the inter- and intra-cell interference but can also exploit the interference channel by transmitting users' data over it. However, the performance gain of CoMP schemes largely depends on the level of synchronization among the nodes, CSI feedback and the backhauling quality. Generally, the CSI feedback of a user from multiple points is needed for CoMP transmissions. Additional information such as phase synchronization for joint

processing with coherent combining is needed for higher level cooperation. Backhaul quality is also important for having the transmit data available at multiple BSs and the exchange of CSI among BSs. Especially for mmWave small cell networks where high-capacity wireless backhaul between small BSs to macro BSs is expected, both the user data transmission and data backhaul are subject to the wireless channel quality. Hence, the overhead in support of CoMP and the accuracy of the feedback are the main implementation issues of CoMP schemes. Practical CoMP performance assessment should consider imperfect CSI, synchronization, and network latency.

3.2 Joint Hybrid Precoding in Cooperative MmWave Systems

5G systems with mmWave small cells will enable CoMP with multi-layer connectivity resulting in much higher data rates compared to current networks. One of the main differences between CoMP in mmWave and sub-6G Hz communications is the beamforming architecture. Equipped with massive antenna arrays, mmWave BSs will choose the hybrid beamforming architecture with reduced number of RF chains to minimize the cost, thus both the analog and digital beamforming need to be jointly designed. Optimal hybrid beamforming design for capacity maximization involves non-convex problems [2, 3], algorithm development for CoMP mmWave communications is required to reduce the complexity of joint beamforming and improve the optimality of currently proposed hybrid beamforming schemes. In addition, CoMP schemes need to exploit mmWave channels' poor penetration to reduce the interference power, but still ensure close to LOS transmissions to the intended users.

In this subsection, we present the system model of a multi-tier cooperative mmWave network where joint processing is possible. Because one of the key features of 5G is the systems' sustainability, joint hybrid precoding schemes are proposed in Paper C to minimize the total power consumption of the network while satisfying a per-user rate constraint.

3.2.1 System Model

We consider the downlink cooperation in a multi-tier mmWave network consisting of M multi-antenna BSs and K single-antenna users. BSs in different tiers have different numbers of antennas, RF chains and maximum RF transmit power. We denote the number of RF chains and the number of antennas at BS m by L_m and N_m, respectively. The precoder at BS m for user k is denoted by $\mathbf{w}_{k,m} = \mathbf{R}_m \mathbf{d}_{k,m}$, where $\mathbf{d}_{k,m} \in \mathbb{C}^{L_m}$ is the digital precoder and $\mathbf{R}_m \in \left\{ \mathbf{R}_m \in \mathbb{C}^{N_m \times L_m} \middle| \left| \mathbf{R}_m^{(i,j)} \right| = \frac{1}{\sqrt{N_m L_m}} \right\}$ is the analog precoder. The analog precoder has an equal magnitude constraint as it is implemented by phase shifters. For the joint processing, a user can receive multiple streams from different BSs

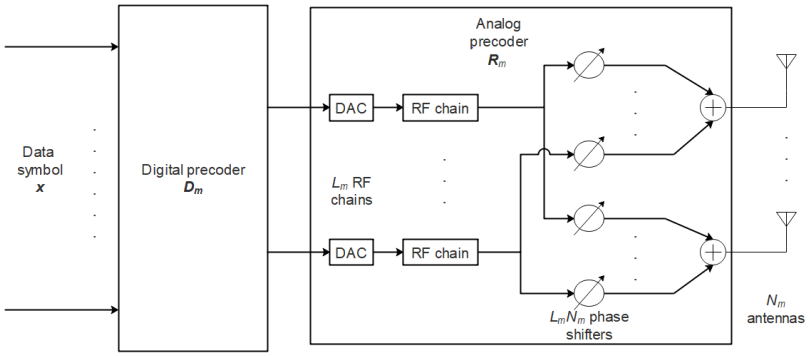

Figure 3.1: The hybrid beamforming architecture.

concurrently, the composite received signal at UE k is given by

$$y_k = \sum_{m=1}^{M} \mathbf{h}_{k,m}\mathbf{R}_m\mathbf{d}_{k,m}x_{k,m} + \sum_{m=1}^{M}\sum_{k'\neq k,k'=1}^{K} \mathbf{h}_{k,m}\mathbf{R}_m\mathbf{d}_{k',m}x_{k',m} + n_k, \tag{3.1}$$

where $\mathbf{h}_{k,m} \in \mathbb{C}^{N_m}$ is the channel vector between user k and BS m, $x_{k,m}$ is the data symbol with $\mathbb{E}[x_{k,m}x_{k,m}^H] = 1$, the second term is the inter-user interference and $n_k \sim \mathcal{CN}(0, \sigma_k^2)$ is the AWGN noise. Note that if BS m is not associated with UE k in the joint transmission, it must satisfy $\mathbf{R}_m\mathbf{d}_{k,m} = \mathbf{0}$.

We assume that the data symbols are mutually independent and the user applies successive interference cancellation to sequentially decode the strongest signal and subtract it from the composite signal. Assuming Gaussian signaling, the achievable spectral efficiency of UE y is given by

$$\eta_k = \log_2\left(1 + \frac{\sum_{m=1}^{M} |\mathbf{h}_{k,m}^H\mathbf{R}_m\mathbf{d}_{k,m}|^2}{I_k + \sigma_k^2}\right), \tag{3.2}$$

where

$$I_k = \sum_{m=1}^{M}\sum_{k'\neq k,k'=1}^{K} \mathbf{d}_{k',m}^H\mathbf{R}_m^H\mathbf{h}_{k,m}\mathbf{h}_{k,m}^H\mathbf{R}_m\mathbf{d}_{k',m} \tag{3.3}$$

is the interference power.

The main difference between the hybrid and the fully-digital beamforming architectures is the hardware and its associated power consumption. To compare the power consumption of the two architectures, we focus on the number of DACs, RF chains and phase shifters needed for each architecture, since they are the most power-consuming components [8]. As shown in Figure 3.1, the hybrid beamforming architecture requires

L_m additional PSs per antenna but $(N_m - L_m)$ less digital-to-analog converters (DACs) and RF chains compared to the fully-digital beamforming architecture. Hence, the total power consumption of the hybrid beamforming architecture at a BS can be modeled by

$$P_m^{\mathrm{HB}} = \Delta_m \sum_{k=1}^{K} ||\mathbf{R}_m \mathbf{d}_{k,m}||^2 + L_m N_m P_{\mathrm{ps}} + L_m \left(P_{\mathrm{DAC}} + P_{\mathrm{RF}}\right) + P_{\mathrm{fix},m}, \tag{3.4}$$

and the total power consumption of the fully-digital beamforming architecture is given by

$$P_m^{\mathrm{FD}} = \Delta_m \sum_{k=1}^{K} ||\mathbf{R}_m \mathbf{d}_{k,m}||^2 + N_m \left(P_{\mathrm{DAC}} + P_{\mathrm{RF}}\right) + P_{\mathrm{fix},m}. \tag{3.5}$$

In (3.4) and (3.5), $\Delta_m \sum_{k=1}^{K} ||\mathbf{R}_m \mathbf{d}_{k,m}||^2$ is the power consumption at the amplifier and Δ_m models the power amplifier inefficiency. Then, $P_{\mathrm{ps}}, P_{\mathrm{DAC}}$ and P_{RF} denote the power consumption of the phase shifters, DACs and RF chains, respectively. Furthermore, $P_{\mathrm{fix},m}$ denotes the power dissipated at various other places, such as the power supply, cooling and backhaul maintenance.

Another mechanism which can greatly increase the power saving is to coordinate BSs' sleep and active mode such that the BS should be operational only when there is data to transmit. Depending on the latency requirement on the deactivation and reactivation, some hardware components need to remain active during the sleep mode. Considering the BS active/sleep mode, the power consumption is modeled by

$$P_m = \begin{cases} P_m^{\mathrm{HB/FD}}, & \text{active mode} \\ a P_m^{\mathrm{HB/FD}}, & a \in [0,1]\ , \text{ sleep mode.} \end{cases} \tag{3.6}$$

Note that in sleep mode, BSs do not serve the users, hence $\Delta_m \sum_{k=1}^{K} ||\mathbf{R}_m \mathbf{d}_{k,m}||^2 = 0$.

To fulfill the target of designing energy-efficient 5G systems, we jointly design the hybrid precoders to minimize the total power consumption of all BSs while guaranteeing the QoS for each user. The joint processing problem is summarized as

$$\mathcal{P} : \min\nolimits_{\mathbf{R}_m \mathbf{d}_{k,m}} \sum_{m=1}^{M} b_m P_m \tag{3.7}$$

$$\text{s.t.} \quad \eta_k \geq \tau_k, \qquad \forall k \tag{3.8}$$

$$\sum_{k=1}^{K} ||\mathbf{R}_m \mathbf{d}_{k,m}||^2 \leq P_{\max,m}, \qquad \forall m \tag{3.9}$$

$$\left|\mathbf{R}_m^{(i,j)}\right| = \frac{1}{\sqrt{N_m L_m}}, \qquad \forall m, i, j. \tag{3.10}$$

where b_m is the weighting parameter for balancing the load of BSs, τ_k is the minimum acceptable spectral efficiency for user k and can be used to ensure fairness among users, and $P_{\max,m}$ is the peak power limit of BS m. The solution to problem $\mathcal{P}$ gives the

analog precoder for each BS and the digital precoder for each BS-user pair. It also reflects the UE association strategy, as the set of associated UEs of BS m is given by $\mathcal{K}_m = \{k|0 \leq k \leq K, ||\mathbf{R}_m \mathbf{d}_{k,m}||^2 > 0\}$ and the set of serving BSs of UE k is given by $\mathcal{M}_k = \{m|0 < m \leq M, ||\mathbf{R}_m \mathbf{d}_{k,m}||^2 > 0\}$.

The optimal solution to Problem $\mathcal{P}$ is not tractable due to the non-convex analog precoder constraint (10). Hence, suboptimal hybrid precoding methods [2–4, 7, 8, 13] are often based on disjoint analog and digital precoders design. In paper C, we decouple Problem $\mathcal{P}$ into an equal gain transmission problem, where analog precoders are found based on maximizing the useful signal power and a relaxed convex semi-definite problem which gives the digital precoders that solve Problem $\mathcal{P}$ conditioned on the analog precoders. The power consumption is compared to that of the fully-digital beamforming architecture for which precoders are obtained by setting $L_m = N_m$ and removing the analog constraint (10) in Problem $\mathcal{P}$.

3.3 MmWave Channel Model

Measurements of mmWave channels have shown that many parameter statistics are different from sub-6 GHz signals. For example, the penetration loss of mmWave signals can be as high as 40 dB for a tinted glass in 28 GHz, and the diffuse scattering from rough surfaces causes large channel variations over short distance [41]. Also, the mmWave signal power can change dramatically from LOS to non-line-of-sight (NLOS) and human blockage can cause more than 40 dB fading [41]. Understanding the mmWave channel characteristics will help researchers to design proper channel modeling, link adaptation and beamforming algorithms for performance enhancement. In this subsection, we present mmWave channel modeling that are commonly used for simulations.

Due to the fact that the angular spread is smaller in mmWave channels compared to lower frequency channels, there may be few dominant multi-path clusters with many subpaths of similar power, delay and angles, the mmWave channel can be modeled by the Saleh-Valenzuela model, where we denote the channel vector between BS m and user k by

$$\mathbf{h}_{k,m} = \sqrt{\frac{l_{k,m} N_m}{N_{\text{cl}} N_{\text{ray}}}} \sum_{i=1}^{N_{\text{cl}}} \sum_{l=1}^{N_{\text{ray}}} \beta_{i,l} \mathbf{a}_m(\alpha_{i,l}). \tag{3.11}$$

Here, $l_{k,m}$ denotes the path loss, N_{cl} is the number of scattering clusters and N_{ray} represents the number of multipaths within a cluster. Also, $\beta_{i,l} \sim \mathcal{CN}(0,1)$ is the amplitude of the l-th path in the i-th cluster and $\mathbf{a}_m(\alpha_{i,l})$ denotes the antenna array response vector evaluated at the angle of departure $\alpha_{i,l}$. Depending on the antenna geometry, various array response vectors have been proposed. For simplicity, we adopt the linear array antennas whose response vector given by

$$\mathbf{a}_m(\alpha_{i,l}) = \frac{1}{\sqrt{N_m}} \left[1, e^{jkd \sin(\alpha_{i,l})}, ..., e^{jkd(N_m - 1) \sin(\alpha_{i,l})}\right]^T, \tag{3.12}$$

where $k = 2\pi/\lambda$, λ is the wavelength, $d = \lambda/2$ is the antenna spacing and $\alpha_{i,l}$ is assumed to follow a truncated Laplace distribution with mean cluster angle $\bar{\alpha}_i \sim \mathcal{U}(\alpha_v^{\min}, \alpha_v^{\max})$ and angular spread σ_{α_i}.

There are numerous large-scale path loss models proposed for mmWave communications. In general, the parameters of the path loss models vary according to the scenarios and the frequency. For mmWave communications, the path loss model should differentiate between LOS and NLOS paths, as the signal power can be significantly different. Here, we present a collection of well adopted path loss models.

- *Path loss model with blocking* [14]: In order to show the difference between LOS and NLOS signal power, the path loss can be modeled as

$$l_{k,m} = \mathbb{I}(p_{\text{LOS}}(d_{k,m}))C_L d_{k,m}^{-\alpha_L} + (1 - \mathbb{I}(p_{\text{NLOS}}(d_{k,m})))C_N d_{k,m}^{-\alpha_N}. \tag{3.13}$$

  Here, $\mathbb{I}(p_L(r))$ is a Bernoulli random variable with LOS probability $p_L(r)$, α_L, α_N and C_L, C_N denote the path loss exponents and path loss at a reference distance for LOS and NLOS links, respectively. In [14], the LOS probability function is given by $p_{\text{LOS}}(d_{k,m}) = e^{-\beta d_{k,m}}$ where β is used to fit the model with different environments. The 3GPP LOS probability models are given by piece-wise functions [43]. The LOS probability is 1 if the distance is smaller than a threshold, otherwise it decays exponentially with distance.

- *Multi-slope path loss model* [44]: Standard Friis path loss model with one path loss exponent lead to unrealistic results in many scenarios, the multi-slope path loss model changes the path loss exponent according to the distance by

$$l_{k,m} = K_n d_{k,m}^{-\alpha_n}. \tag{3.14}$$

  Here, $d_{k,m}$ is the distance between user k and BS m, $K_n = \prod_{i=1}^{n} R_i^{\alpha_i - \alpha_{i-1}}$ and R_i is a critical distance beyond which the path loss exponent changes.

- *3GPP-based path loss model* [43]: This path loss model is defined separately for LOS and NLOS paths and is based on field measurements. For example, the LOS model of urban micro-cells is given by

$$l_{k,m}^{\text{LOS}} = \begin{cases} \text{PL}_1, & 10\text{m} \leq d_{k,m} \leq d \\ \text{PL}_2, & d \leq d_{k,m} \leq d_{\max} \end{cases} \tag{3.15}$$

  where

$$\text{PL}_i = A_i + B_i \log_{10}(d_{k,m}) + 20\log_{10}(f_c) + C_i, \qquad i = \{1, 2\}. \tag{3.16}$$

  Here, $d, d_{\max}, A_i, B_i, C_i$ are cell specific parameters and f_c is the carrier frequency.

- *Probabilistic path loss model* [15]: In order to generalize the path loss model to average the LOS and NLOS conditions, a weighting parameter, which is a function of the LOS probability, can be given to the two path loss models and we have

$$l_{k,m} = p_{\text{LOS}}(d_{k,m})\text{PL}_{\text{LOS}} + (1 - p_{\text{LOS}}(d_{k,m}))\,\text{PL}_{\text{NLOS}}. \tag{3.17}$$

  Here, the LOS/NLOS path loss models and LOS probability may be chosen according to the preciously mentioned models.

Chapter 4

Conclusions and Future Work

4.1 Contributions

This thesis analyzes the coverage performance of unstructured dense networks and the joint hybrid beamforming scheme for cooperative mmWave networks. The list of the papers and a summary of the contributions are given as follows.

1. **Paper A: "Equal Gain Combining in Poisson Networks with Spatially Correlated Interference Signals"**

   We study the successful reception probability and the area spectral efficiency (ASE) of equal gain receivers in a network where transmitters are distributed according to a PPP. Considering spatially correlated interference signals, we derive exact analytical expression of the successful reception probability for two receive antennas and tight approximations for more than two receive antennas. Also, we give an approximation for the optimal transmitter density maximizing the ASE. The results show that the fully-correlated case where interference on different antennas are from the same set of transmitters gives pessimistic successful reception probability, while the uncorrelated case is optimistic.

2. **Paper B: "Coverage Analysis for Millimeter Wave Uplink Cellular Networks with Partial Zero-Forcing Receivers"**

   This paper considers interference management and useful signal enhancement in the uplink transmission of small-cell mmWave networks. Taking blockages into account, we analyze the coverage performance of the partial-zero-forcing (PZF) receiver which utilizes a number of antennas to cancel out the strongest uplink interferers and uses the rest of the antennas for boosting the useful signal. Using stochastic geometry, we derive analytical expressions for the coverage probability of the PZF receiver under a LOS probability function based path loss model. For a broad range of parameter settings, the maximum coverage probability is achieved by using most antennas for array gain and only canceling a few strongest interferers.

3. **Paper C: "Coordinated Hybrid Precoding for Energy-efficient Millimeter Wave Systems"**

   The previous papers focus on the system performance analysis of multi-receive antenna techniques. In this paper, we develop a joint downlink beamforming scheme of cooperative BSs with multiple transmit antennas. By allowing joint transmissions from multiple BSs, we jointly optimize over the hybrid precoders and the BSs sleep/active modes such that the total power consumption is minimized with per-user quality-of-service constraints. We present a decoupled hybrid beamforming scheme where the analog precoders are designed based on the equal gain transmission method and the digital precoders are found by solving a convex semidefinite problem. We define fairly realistic models for the hardware power consumption and the channel blocking probabilities to compare the performance of our scheme with the fully-digital precoding scheme and to assess the value of BS cooperation. The results show that our proposed method results in almost the same RF transmit power as the fully-digital precoding scheme while saving considerable hardware power due to the reduced number of RF chains and digital-to-analog converters. Moreover, the network densification is shown to further reduce the total power consumption through the optimized cooperative BS active/sleeping mode selection.

4.2 Future Work

In this thesis, we have investigated the SINR distribution and the joint transmission schemes in mmWave networks. The results of the SINR distribution can be extended in many ways, including more realistic heterogeneous topologies and other MIMO transmission and reception techniques. Our baseline model for the joint transmission is based on a fully-connected hybrid beamforming architecture and perfect CSI. To further reduce the power consumption and the hardware complexity, partially-connected architectures where each RF chain is connected to a subset of the antennas and hybrid architectures with low-resolution ADCs are promising areas to investigate. Another direction is to consider more realistic constraints. Given the importance of CSI, errors in the estimates of the angles of departure or arrival may significantly affect the narrow beams' direction in mmWave communications, it is interesting to study the effect of limited angular information to other BSs on the system performance. Also, since each RF chain can not be allocated with arbitrary power, the per-RF chain power constraint can be interesting to included in the CoMP design problem. Since mmWave BSs are expected to be densely deployed, wireless backhaul is a promising technology for practical deployment of mmWave BSs. Small BSs with wireless backhaul to macro BSs results in a multi-hop network, the study of the overall throughput and the energy efficiency considering both access links and backhaul links can provide valuable guidelines for developing 5G networks.

4.3 List of Related Publications

The related contributions, which are not included in this thesis, are listed below.

[J1] **C. Fang**, B. Makki, T. Svensson, "On the performance of the Poisson-point-process-based networks with no channel state information feedback", in *IET Communications*, Volume 10, Issue 15, p. 2018-2024, Oct. 2016.

[J2] B. Makki, **C. Fang**, T. Svensson, M. Nasiri-Kenari and M. Zorzi, "Delay-sensitive area spectral efficiency: A performance metric for delay-constrained green networks," in *IEEE Trans. Commun.*, vol. 65, no. 6, pp. 2467-2480, June 2017.

[C1] **C. Fang**, B. Makki, T. Svensson, "HARQ in Poisson point process-based heterogeneous networks", in *IEEE Vehicular Technology Conference (VTC2015-Spring)*, 2015, Glasgow, Scotland.

[C2] B. Makki, **C. Fang**, T. Svensson, M. Nasiri-Kenari, "On the performance of amplifier-aware dense networks: Finite block-length analysis", in *International Conference on Computing, Networking and Communications (ICNC 2016), Workshop on Computing, Networking and Communications (CNC)*, Kauai, Hawaii, USA, Feb. 2016.

[C3] X. Chen, **C. Fang**, Y. Zou, A. Wolfgang and T. Svensson, "Beamforming MIMO-OFDM systems in the presence of phase noises at millimeter-Wave frequencies" in *2017 IEEE Wireless Communications and Networking Conference Workshops (WCNCW)*, San Francisco, CA, 2017, pp. 1-6.

[R1] M. Hunukumbure, M. Castañeda, R. D'Errico, T. Svensson, P. Zetterberg, A. Wolfgang, A. Westlund, Y. Qi, Y. Wang, P. Baracca, D. Ferling, H. Halbauer, M. Iwanow, N. Vucic, J. Luo, L. Dussopt, A. Clemente, B. Makki, **C. Fang**, G. Durisi, Y. Zou, S. Armour, W. Yuan, U. Gustavsson, M. Fresia, H. Miao, D. T. Phan Huy, P. Ratajczak, H. Wang, EU H2020 ICT-2014-2-671650 mmMAGIC, "D5.1 Initial multi-node and antenna transmitter and receiver architectures and schemes", Mar 2016.

[R2] D.T. Phan Huy, P. Ratajczak, K. Haneda, J. Järveläinen, A. Karttunen, M. Beach, E. Mellios, D. Kong, B. Bulut, A. Goulianos, W. Yuan, S. Armour, M. Castañeda, M. Iwanow, N. Vucic, J. Luo, Y. Zou, P. Baracca, S. Wesemann, M. Hunukumbure, Y. Qi, C. Kim, Honglei Miao, M. Filippou, K. Roth, U. Gustavsson, T. Svensson, B. Makki, **C. Fang**, G. Durisi, R. D'Errico, A. Clemente, A. Wolfgang, X. Chen, EU H2020 ICT-2014-2-671650 mmMAGIC "D5.2 Final multi-node and multi-antenna transmitter and receiver architectures and schemes", Jun 2017.

References

[1] "Ericsson mobility report," Ericsson, Nov. 2018. [Online]. Available: https://bit.ly/2SSxYL3

[2] J. G. Andrews, S. Buzzi, W. Choi, S. V. Hanly, A. Lozano, A. C. K. Soong, and J. C. Zhang, "What will 5G be?" *IEEE J. Sel. Areas Commun.*, vol. 32, no. 6, pp. 1065–1082, Jun. 2014.

[3] A. Osseiran, J. F. Monserrat, and P. Marsch, *5G Mobile and Wireless Communications Technology*. Cambridge University Press, 2016.

[4] T. S. Rappaport, S. Sun, R. Mayzus, H. Zhao, Y. Azar, K. Wang, G. N. Wong, J. K. Schulz, M. Samimi, and F. Gutierrez, "Millimeter wave mobile communications for 5G cellular: It will work!" *IEEE Access*, vol. 1, pp. 335–349, 2013.

[5] T. L. Marzetta, "Noncooperative cellular wireless with unlimited numbers of base station antennas," *IEEE Trans. Wireless Commun.*, vol. 9, no. 11, pp. 3590–3600, Nov. 2010.

[6] Int Telecom Union - Radiocom Sector (ITU-R), Resolution 809, World Radiocommunication Conference, Geneva, Nov. 2015.

[7] "3rd Generation Partnership Project; Technical Specification Group Radio Access Network; New Bands and Band Combinations for Frequency Range ; (Release 16)," 3GPP, Mar. 2019. [Online]. Available: https://bit.ly/2YEzvD5

[8] J. Vehmas, J. Jarvelainen, S. L. H. Nguyen, R. Naderpour, and K. Haneda, "Millimeter-wave channel characterization at Helsinki airport in the 15, 28, and 60 GHz bands," in *IEEE 84th Vehicular Technology Conference (VTC-Fall)*, Sept 2016, pp. 1–5.

[9] T. S. Rappaport, G. R. MacCartney, M. K. Samimi, and S. Sun, "Wideband millimeter-wave propagation measurements and channel models for future wireless communication system design," *IEEE Trans. Commun.*, vol. 63, no. 9, pp. 3029–3056, Sept 2015.

[10] M. K. Samimi, T. S. Rappaport, and G. R. MacCartney, "Probabilistic omnidirectional path loss models for millimeter-wave outdoor communications," *IEEE Wireless Commun. Lett.*, vol. 4, no. 4, pp. 357–360, Aug. 2015.

[11] O. E. Ayach, S. Rajagopal, S. Abu-Surra, Z. Pi, and R. W. Heath, "Spatially sparse precoding in millimeter wave MIMO systems," *IEEE Trans. Wireless Commun.*, vol. 13, no. 3, pp. 1499–1513, Mar. 2014.

[12] X. Gao, L. Dai, S. Han, C. L. I, and R. W. Heath, "Energy-efficient hybrid analog and digital precoding for mmwave MIMO systems with large antenna arrays," *IEEE J. Sel. Areas Commun.*, vol. 34, no. 4, pp. 998–1009, April 2016.

[13] J. Mo, A. Alkhateeb, S. Abu-Surra, and R. W. Heath, "Hybrid architectures with few-bit ADC receivers: Achievable rates and energy-rate tradeoffs," *IEEE Trans. Wireless Commun.*, vol. 16, no. 4, pp. 2274–2287, April 2017.

[14] R. Méndez-Rial, C. Rusu, N. González-Prelcic, A. Alkhateeb, and R. W. Heath, "Hybrid MIMO architectures for millimeter wave communications: Phase shifters or switches?" *IEEE Access*, vol. 4, pp. 247–267, 2016.

[15] J. Mo and R. W. Heath, "Capacity analysis of one-bit quantized MIMO systems with transmitter channel state information," *IEEE Trans. Signal Process.*, vol. 63, no. 20, pp. 5498–5512, Oct 2015.

[16] C. Rusu, R. Mèndez-Rial, N. González-Prelcic, and R. W. Heath, "Low complexity hybrid precoding strategies for millimeter wave communication systems," *IEEE Trans. Wireless Commun.*, vol. 15, no. 12, pp. 8380–8393, Dec. 2016.

[17] A. Michaloliakos, W. C. Ao, and K. Psounis, "Joint user-beam selection for hybrid beamforming in asynchronously coordinated multi-cell networks," in *2016 Information Theory and Applications Workshop (ITA)*, Jan. 2016, pp. 1–10.

[18] S. Sun, T. S. Rappaport, M. Shafi, and H. Tataria, "Analytical framework of hybrid beamforming in multi-cell millimeter-wave systems," *IEEE Trans. Wireless Commun.*, vol. 17, no. 11, pp. 7528–7543, Nov 2018.

[19] J. G. Andrews, H. Claussen, M. Dohler, S. Rangan, and M. C. Reed, "Femtocells: Past, present, and future," *IEEE J. Sel. Areas Commun.*, vol. 30, no. 3, pp. 497–508, April 2012.

[20] M. Kamel, W. Hamouda, and A. Youssef, "Ultra-dense networks: A survey," *IEEE Communications Surveys Tutorials*, vol. 18, no. 4, pp. 2522–2545, 2016.

[21] "3GPP work items on H(e)NB," 3GPP, Jun. 2014. [Online]. Available: https://goo.gl/gkFGkN

[22] X. Ge, H. Cheng, M. Guizani, and T. Han, "5G wireless backhaul networks: challenges and research advances," *IEEE Network*, vol. 28, no. 6, pp. 6–11, Nov 2014.

[23] A. Ghosh, N. Mangalvedhe, R. Ratasuk, B. Mondal, M. Cudak, E. Visotsky, T. A. Thomas, J. G. Andrews, P. Xia, H. S. Jo, H. S. Dhillon, and T. D. Novlan, "Heterogeneous cellular networks: From theory to practice," *IEEE Commun. Mag.*, vol. 50, no. 6, pp. 54–64, June 2012.

[24] "3rd Generation Partnership Project; Technical Specification Group Radio Access Network; Study on Integrated Access and Backhaul; (Release 16)," 3GPP TR 38.874, Dec. 2018. [Online]. Available: https://bit.ly/2YEzvD5

[25] H. S. Jo, Y. J. Sang, P. Xia, and J. G. Andrews, "Heterogeneous cellular networks with flexible cell association: A comprehensive downlink SINR analysis," *IEEE Trans. Wireless Commun.*, vol. 11, no. 10, pp. 3484–3495, October 2012.

[26] J. G. Andrews, F. Baccelli, and R. K. Ganti, "A tractable approach to coverage and rate in cellular networks," *IEEE Trans. Commun.*, vol. 59, no. 11, pp. 3122–3134, Dec. 2011.

[27] M. Haenggi and R. K. Ganti, *Interference in large wireless networks.* Now Publishers Inc, 2009.

[28] M. Haenggi, *Stochastic Geometry for Wireless Networks.* Cambridge University Press, 2012.

[29] Q. Ye, M. Al-Shalash, C. Caramanis, and J. G. Andrews, "On/off macrocells and load balancing in heterogeneous cellular networks," in *2013 IEEE Global Communications Conference (GLOBECOM)*, Dec 2013, pp. 3814–3819.

[30] S. Singh, X. Zhang, and J. G. Andrews, "Joint rate and SINR coverage analysis for decoupled uplink-downlink biased cell associations in hetnetss," *IEEE Trans. Wireless Commun.*, vol. 14, no. 10, pp. 5360–5373, Oct 2015.

[31] "3rd Generation Partnership Project; CoMP operation for LTE with non-ideal backhaul (Release 12) ," 3GPP TR 36.874, Dec. 2013.

[32] "3rd Generation Partnership Project; CoMP operation for LTE physical layer aspects (Release 11)," 3GPP TR 36.819, Sep. 2013.

[33] M. Hong, R. Sun, H. Baligh, and Z. Q. Luo, "Joint base station clustering and beamformer design for partial coordinated transmission in heterogeneous networks," *IEEE J. Sel. Areas Commun.*, vol. 31, no. 2, pp. 226–240, February 2013.

[34] J. Li, E. Björnson, T. Svensson, T. Eriksson, and M. Debbah, "Joint precoding and load balancing optimization for energy-efficient heterogeneous networks," *IEEE Trans. Wireless Commun.*, vol. 14, no. 10, pp. 5810–5822, Oct 2015.

[35] S. Schwarz and M. Rupp, "Exploring coordinated multipoint beamforming strategies for 5G cellular," *IEEE Access*, vol. 2, pp. 930–946, 2014.

[36] S. Sun, T. S. Rappaport, and M. Shaft, "Hybrid beamforming for 5g millimeter-wave multi-cell networks," in *IEEE Conference on Computer Communications Workshops (INFOCOM WKSHPS)*, Apr. 2018, pp. 589–596.

[37] D. Gesbert, S. Hanly, H. Huang, S. S. Shitz, O. Simeone, and W. Yu, "Multi-cell MIMO cooperative networks: A new look at interference," *IEEE J. Sel. Areas Commun.*, vol. 28, no. 9, pp. 1380–1408, December 2010.

[38] B. Makki, T. Eriksson, and T. Svensson, "On an HARQ-based coordinated multi-point network using dynamic point selection," *EURASIP Journal on Wireless Communications and Networking*, vol. 2013:209, 2013.

[39] T. R. Lakshmana, B. Makki, and T. Svensson, "Frequency allocation in non-coherent joint transmission CoMP networks," in *IEEE International Conference on Communications Workshops (ICC).*, Sydney, NSW, June 2014, pp. 610–615.

[40] W. Ni and X. Dong, "Hybrid block diagonalization for massive multiuser MIMO systems," *IEEE Trans. Commun.*, vol. 64, no. 1, pp. 201–211, Jan. 2016.

[41] T. S. Rappaport, Y. Xing, G. R. MacCartney, A. F. Molisch, E. Mellios, and J. Zhang, "Overview of millimeter wave communications for fifth-generation (5G) wireless networksŮwith a focus on propagation models," *IEEE Trans. Antennas Propag.*, vol. 65, no. 12, pp. 6213–6230, Dec. 2017.

[42] T. Bai and R. W. Heath, "Coverage and rate analysis for millimeter-wave cellular networks," *IEEE Trans. Wireless Commun.*, vol. 14, no. 2, pp. 1100–1114, Feb. 2015.

[43] "3rd Generation Partnership Project; Technical Specification Group Radio Access Network; Study on channel model for frequency spectrum above 6 GHz (Release 15)," TR 38.900, 3GPP, Jun. 2018.

[44] X. Zhang and J. G. Andrews, "Downlink cellular network analysis with multi-slope path loss models," *IEEE Trans. Commun.*, vol. 63, no. 5, pp. 1881–1894, May 2015.

[45] "Measurement results and final mmMAGIC channel models," Deliverable D2.2, mmMAGIC, May 2017.

Part II

Included papers